



Published in final edited form as:

Nature. ; 487(7406): 183–189. doi:10.1038/nature11160.

Anhedonia requires MC4 receptor-mediated synaptic adaptations in nucleus accumbens

Byung Kook Lim¹, Kee Wui Huang¹, Brad A. Grueter¹, Patrick E. Rothwell¹, and Robert C. Malenka¹

¹Nancy Pritzker Laboratory, Department of Psychiatry and Behavioral Sciences, Stanford University School of Medicine, 265 Campus Drive, Stanford CA 94305, USA

Abstract

Chronic stress is a strong diathesis for depression in humans and is used to generate animal models of depression. It commonly leads to several major symptoms of depression including dysregulated feeding behavior, anhedonia, and behavioral despair. Although hypotheses defining the neural pathophysiology of depression have been proposed, the critical synaptic adaptations in key brain circuits that mediate stress-induced depressive symptoms remain poorly understood. Here we show that chronic stress decreases the strength of excitatory synapses on D1 dopamine receptor-expressing nucleus accumbens medium spiny neurons due to activation of melanocortin 4 receptors (MC4Rs). Stress-elicited increases in behavioral measurements of anhedonia, but not increases in measurements of behavioral despair, are prevented by blocking these MC4R-mediated synaptic changes *in vivo*. These results establish that stress-elicited anhedonia requires a neuropeptide-triggered, cell type-specific synaptic adaptation in the nucleus accumbens and that distinct circuit adaptations mediate other major symptoms of stress-elicited depression.

The neural mechanisms governing food intake have been extensively studied and a host of genetic and environmental factors influence this behavior in large part by affecting the levels of neuropeptides that act on hypothalamic circuitry^{1–3}. In addition there are strong links between brain circuits mediating feeding behavior and those responsible for appetitive motivation and “reward” as evidenced, for example, by the simple fact that the palatability and reward value of food are greatly influenced by satiety perception^{1–5}. Although two common symptoms of depression, dysregulated feeding behavior and anhedonia, likely involve maladaptive integration and functioning of these brain circuits^{1–3, 6}, the mechanisms by which neuropeptides that regulate food intake contribute to symptoms of depression are poorly understood.

Users may view, print, copy, download and text and data- mine the content in such documents, for the purposes of academic research, subject always to the full Conditions of use: http://www.nature.com/authors/editorial_policies/license.html#terms

Correspondence to: R. Malenka, Department of Psychiatry and Behavioral Sciences, 265 Campus Drive, Room G1021, Stanford University School of Medicine, Stanford, CA 94305, Tel. 650-724-2730, Fax. 650-724-2753, malenka@stanford.edu.

Author Contributions The study was designed and results were interpreted by B.K.L. and R.C.M. with assistance from K.W.H., B.A.G., and P.E.R. Virus injections and RV production were performed by B. K. L. and K.W. H. All experiments were performed and analyzed by B.K.L. with assistance from B.A.G. for electrophysiology experiments and P.E.R. for conditioned place preference assays. The manuscript was written by B.K.L. and R.C.M. and edited by all authors.

A key brain region regulating feeding behavior and energy homeostasis in response to metabolic rates and emotional status is the arcuate nucleus (ARC) of the hypothalamus¹⁻³. It contains two major subpopulations of neurons that secrete orexigenic or anorexigenic neuropeptides, including neuropeptide Y or α -melanocyte-stimulating hormone (α -MSH), respectively. The role of such neuropeptides in feeding behavior has largely focused on hypothalamic circuitry while their actions in circuits mediating appetitive motivation are much less well understood. Here, we explore the role of α -MSH signaling in the nucleus accumbens (NAc), a key component of the brain's "reward" circuitry^{4,5}, in chronic stress-elicited behavioral changes that are commonly used as indices of depression in rodents. We focused on the potential role of α -MSH acting specifically in the NAc in mediating stress-induced depression symptoms because ARC neurons expressing α -MSH are activated by stress⁷, MC4Rs are expressed in the NAc⁸, and pharmacological inhibition of MC4Rs influences a variety of stress-induced behaviors related to anxiety, addiction and depression⁸⁻¹⁰.

α -MSH decreases synaptic strength in NAc D1-MSNs

To test whether α -MSH influences synaptic function in the NAc, we applied α -MSH to NAc slices and examined excitatory synaptic transmission using slices prepared from BAC transgenic mice expressing tdTomato in D1 dopamine receptor-expressing MSNs (D1-MSNs) and EGFP in D2 dopamine receptor-expressing MSNs (D2-MSNs)¹¹ (Fig. 1a). These MSN subtypes have distinct properties^{12, 13} and different roles in reward-related learning^{14, 15}. The paired-pulse ratios of excitatory postsynaptic currents (EPSCs), which inversely correlate with neurotransmitter release probability, were not affected by α -MSH in either D1-MSNs or D2-MSNs (Supplementary Fig. 1). In contrast, a measure of changes in postsynaptic function, the ratio of the amplitude of AMPAR-mediated EPSCs to N-methyl-D-aspartate receptor (NMDAR)-mediated EPSCs (AMPA/NMDAR ratio)¹⁶ was decreased by α -MSH in D1-MSNs (Fig. 1b, c) but not D2-MSNs (Fig. 1d,e). AMPAR-mediated miniature EPSC (mEPSC) frequency was unaffected by α -MSH but mEPSC amplitude was decreased (Fig. 1f-i) suggesting that α -MSH caused a change in the number and/or biophysical properties of synaptic AMPARs.

Because the stoichiometry of AMPARs in NAc MSNs can be modulated by withdrawal from cocaine¹⁷ we examined whether α -MSH influenced the voltage-dependent properties of AMPAR EPSCs, an indication of the relative proportion of GluA2-containing and GluA2-lacking AMPARs since these latter AMPARs exhibit inward rectification¹⁸. While AMPAR EPSCs in control D1-MSNs exhibited linear current/voltage relationships, AMPAR EPSCs in D1-MSNs exposed to α -MSH showed inward rectification (Fig. 1j). This suggests that α -MSH caused an increase in the proportion of synaptic AMPARs lacking GluA2 compared to GluA2-containing AMPARs. To test this conclusion, we applied 1-naphthylacetylspermine (Naspm, 200 μ M), a selective blocker of GluA2-lacking AMPARs. This manipulation had minimal effects on AMPAR EPSCs in control D1-MSNs but caused ~50% decrease in AMPAR EPSCs in D1-MSNs that had been exposed to α -MSH (Fig. 1k). In contrast, α -MSH did not affect the stoichiometry of synaptic AMPARs in D2-MSNs (Fig. 1l, m). These results suggest that α -MSH causes a greater loss of GluA2-containing AMPARs from synapses on D1-MSNs relative to any pre-existing GluA2-lacking synaptic

AMPA receptors. Alternatively, endocytosed GluA2-containing AMPARs may have been replaced by GluA2-lacking AMPARs but this exchange could not be one for one since GluA2-lacking AMPARs have higher conductance than GluA2-containing AMPARs¹⁸. The cell type-specific effects of α -MSH are consistent with the preferential expression of MC4Rs in D1-MSNs⁸. Differences in dopamine receptor expression between D1-MSNs and D2-MSNs are not important for the cell type-specific actions of α -MSH because incubation of slices in D1 and D2 receptor antagonists (SCH23390, 5 μ M; raclopride, 5 μ M) had no effect on the decrease in AMPAR/NMDAR ratios elicited by α -MSH in D1-MSNs (control cells, $n=5$; α -MSH treated cells, $n=5$; data not shown).

Stress decreases synaptic strength in D1-MSNs via MC4Rs

Brain regions involved in feeding behavior, including lateral hypothalamus and ARC, send projections to the NAc¹⁹. However, the specific hypothalamic cell populations that project to NAc have not been definitively identified. To determine whether α -MSH expressing ARC neurons send axons to the NAc, we generated rabies viruses (RVs) in which the glycoprotein is replaced by fluorophores including EGFP (RV-EGFP) and tdTomato (RV-tdTomato). These RVs are taken up by presynaptic terminals and retrogradely transported to somas where they are transduced but cannot be passed onto other synaptically connected neurons²⁰. Thus, they specifically label neurons that send axonal projections directly to the site of injection (Supplementary Fig. 2). Injection of RV-EGFP into NAc core and RV-tdTomato into dorsal striatum resulted in robust EGFP expression in ARC neurons but no tdTomato expression (Fig. 2a). Immunostaining for α -MSH revealed that a subpopulation of EGFP-expressing ARC neurons expressed α -MSH (Fig. 2b; Supplementary Fig. 3). These results demonstrate that a population of α -MSH expressing neurons in ARC project directly to the NAc.

Depression commonly affects appetite and MC4R antagonists ameliorate stress-induced symptoms of depression in rodents^{9, 10}. Furthermore, chronic restraint stress increases the number of c-fos positive ARC neurons, which produce α -MSH⁷. Therefore, we hypothesized that stress-induced increases in α -MSH/MC4R signaling in NAc D1-MSNs would cause synaptic adaptations that perturb the rewarding value of food and thus are important for mediating changes in appetite during chronic stress. An 8 day restraint stress decreased body weight (Fig. 2c) due to decreased food intake (Supplementary Fig. 4) and elicited an increase in NAc MC4R levels (Fig. 2d, e). Recordings from NAc slices prepared from chronically stressed animals revealed that D1-MSN AMPAR/NMDAR ratios were decreased compared to those from non-stressed animals (Fig. 2f, g) while AMPAR/NMDAR ratios in D2-MSNs were unaffected by chronic stress (Fig. 2h, i). Furthermore, D1-MSN AMPAR EPSCs in slices from stressed animals exhibited inward rectification (Fig. 2j; Supplementary Fig. 5) and were decreased by Nasp^m (Fig. 2k) whereas D2-MSN AMPAR EPSCs exhibited minimal rectification and minimal sensitivity to Nasp^m (Fig. 2l, m). Thus, the synaptic adaptations in NAc MSNs caused by chronic stress precisely mimic those caused by α -MSH application.

To directly test whether α -MSH signaling via activation of MC4Rs mediated the synaptic changes and weight loss caused by chronic restraint stress we generated a shRNA to MC4Rs

(Supplementary Fig. 6) and expressed it *in vivo* in NAc MSNs using an adeno-associated virus (AAV-MC4R-shRNA) (Fig. 3a, b). This caused a robust depletion of endogenous MC4Rs (Fig. 3c) which effectively prevented the rectification of D1-MSN AMPAR EPSCs normally caused by α -MSH application (Fig. 3d, e). Two weeks after NAc virus injection we subjected animals to chronic restraint stress and found that knockdown of NAc MC4Rs prevented weight loss and the decrease in food intake whereas injections of a control AAV expressing GFP did not (Fig. 3f; Supplementary Fig. 4). Furthermore, the increase in rectification of D1-MSN AMPAR EPSCs caused by chronic stress did not occur in cells expressing MC4R shRNA whereas this increase still occurred in D1-MSNs infected with control AAV (Fig. 3g, h). Expression of MC4R shRNA in control animals had no detectable effect on AMPAR/NMDAR ratios or AMPAR EPSC rectification (data not shown). These results demonstrate that activation of MC4Rs in NAc is required for chronic stress induced weight loss and support the hypothesis that the MC4R-induced synaptic adaptations are also required.

α -MSH and stress occlude LTD in NAc D1-MSNs

To test whether the decrease in AMPAR EPSCs and the change in AMPAR stoichiometry caused by α -MSH activation of MC4Rs in D1-MSNs are in fact required for stress induced weight loss, it was necessary to understand the mechanisms underlying these synaptic changes. Because NMDAR-triggered long-term depression (LTD) in many cell types, including NAc MSNs, involves endocytosis of AMPARs^{16, 21} and GluA2 is important for this process^{22,23}, we hypothesized that MC4R activation elicits AMPAR endocytosis and therefore reduces LTD via occlusion. Consistent with this proposal, NMDAR-dependent LTD in D1-MSNs was reduced following application of α -MSH (Fig. 4a). This form of LTD was also reduced in NAc D1-MSNs in slices prepared from chronically stressed animals, an effect that was prevented by *in vivo* knockdown of MC4Rs (Fig. 4b). Consistent with previous results, LTD was unaffected in D2-MSNs recorded from these same NAc slices (Fig. 4c).

If MC4R activation in NAc during chronic stress leads to synaptic modifications that are the same as those during NMDAR-dependent LTD, then LTD should be accompanied by a change in AMPAR stoichiometry. To test this prediction we induced LTD in D1-MSNs and then applied Nasp^m (Fig. 4d), which caused a depression of AMPAR EPSCs (Fig. 4d, e) that was similar to that caused by prior application of α -MSH (Fig. 4f). The Nasp^m-induced depression of AMPAR EPSCs in D1-MSNs also occurred in slices prepared from chronically stressed animals, an effect that was prevented by *in vivo* knockdown of MC4Rs (Fig. 4f).

The results presented thus far suggest that NMDAR-dependent LTD and the synaptic changes induced by MC4R activation are due to the endocytosis of GluA2-containing AMPARs. To test this prediction, we generated AAVs expressing a peptide based on the C-terminal tail of GluA2 (G2CT-Pep) that prevents the endocytosis of AMPARs (Fig. 4g)^{21, 22-23}. *In vivo* expression of this peptide strongly reduced LTD in D1-MSNs whereas expression of a control peptide (Con-Pep) did not (Fig. 4h). This peptide provided a manipulation that permitted a direct test of whether the stress-induced synaptic adaptations

in D1-MSNs, like activation of MC4Rs, are required for the associated weight loss. Consistent with this hypothesis, expression of G2CT-Pep in NAc prevented stress-induced weight loss and decrease in food intake, both of which occurred in animals in which the Con-Pep was expressed in NAc (Fig. 4i; Supplementary Fig. 4).

Although we have demonstrated that MC4R activation in NAc D1-MSNs due to α -MSH application and chronic stress decrease AMPAR-mediated synaptic responses, these manipulations may also affect NMDARs in a manner that influences circuit function and synaptic plasticity. However, neither application of α -MSH nor chronic stress affected the time course of decay of dual component EPSCs at +40 mV in D1-MSNs, the voltage-dependence of NMDAR EPSCs, or the size of NMDAR EPSCs as a function of input strength (Supplementary Fig. 7). These results demonstrate that neither α -MSH nor chronic stress detectably affect NMDAR-mediated synaptic transmission. Furthermore, the reduction of LTD in D1-MSNs by prior incubation of NAc slices with α -MSH does not require NMDAR activation (Supplementary Fig. 7).

How might MC4R activation cause endocytosis of GluA2-containing AMPARs? MC4Rs are coupled to Gs and generate increases in cAMP levels²⁴. Because α -MSH caused changes in synaptic AMPARs similar to those caused by activation of the cAMP-activated postsynaptic protein Epac2 (exchange protein directly activated by cAMP) in cultured neurons²⁵ we examined whether application of the cAMP analog, 8-CPT [8-(4-chlorophenylthio)-2'-O-methyladenosine-3',5'-cyclic monophosphate] mimicked the synaptic effects of α -MSH. (8-CPT is used to study Epac function because it activates Epac but not PKA²⁶.) Application of 8-CPT caused a decrease in the AMPAR/NMDAR ratio in D1-MSNs similar to that caused by α -MSH as well as the same change in AMPAR stoichiometry (Supplementary Fig. 8). Furthermore, the depression of D1-MSN AMPAR EPSCs caused by 8-CPT was reduced by prior incubation of slices with α -MSH (Supplementary Fig. 8). 8-CPT application also decreased the subsequent generation of LTD (Supplementary Fig. 8). These findings suggest that α -MSH activation of MC4Rs in NAc D1-MSNs leads to depression of AMPAR-mediated synaptic transmission via cAMP-dependent activation of Epac2.

Behavioral consequences of synaptic changes in NAc

We have presented evidence that activation of MC4Rs in NAc D1-MSNs and the consequent synaptic adaptations are required for one major consequence of the chronic stress protocol, anorexia leading to weight loss. Prevention of stress-induced weight loss by expression of MC4R shRNA and G2CT-Pep in the NAc was not due to these manipulations independently causing abnormal weight gain (Supplementary Fig. 9). Do other behavioral manifestations of chronic stress, in particular behavioral changes used to define depression in rodents^{27, 28}, also require MC4R-mediated synaptic changes in D1-MSNs? To address this question, we performed additional depression-associated behavioral tests in control mice, mice subjected to chronic restraint stress and chronically stressed mice in which the NAc was injected with AAVs expressing GFP, MCR4 shRNA, G2CT-Pep or Con-Pep. The sucrose preference test (SPT) is a commonly used measure of anhedonia in rodent models of depression²⁷. As expected mice subjected to chronic restraint stress exhibited decreased

preference for the sucrose solution (Fig. 5a). This behavioral adaptation was prevented by expression of either MC4R-shRNA or G2CT-Pep in NAc but not by expression of GFP nor Con-Pep (Fig. 5a). Expression of MC4R shRNA in NAc of control animals had no effect on the SPT (data not shown). These results suggest that anhedonia elicited by chronic restraint stress, as defined by the SPT, requires the synaptic adaptations caused by MC4R activation in NAc D1-MSNs.

Surprisingly, two other commonly used behavioral measures of “depression” that reflect behavioral despair, the Porsolt forced swim test and the tail suspension test^{27, 28}, were unaffected by the molecular manipulations that prevented stress-induced weight loss and decrease in sucrose preference. All animals subjected to chronic restraint stress, independent of the virus injected into NAc, showed increased immobility in tail suspension tests (Fig. 5b) as well as decreased latency to initiation of floating (Fig. 5c) and increased total time floating (Fig. 5d) in forced swim tests. Expression of MC4R shRNA in control animals had no significant effect on any of these behavioral measures (data not shown).

In all experiments, MC4R shRNA was expressed in both D1-MSNs and D2-MSNs. Although there were no detectable synaptic effects of α -MSH or chronic stress in NAc D2-MSNs, it is conceivable that in both cell types MC4R shRNA could have off-target effects that contribute to its behavioral actions. To directly test whether knockdown of only MC4Rs specifically in NAc D1-MSNs was responsible for reversing stress-induced weight loss and decrease in sucrose preference, we performed a cell type-specific rescue experiment. We generated an AAV that expressed MC4R shRNA together with a double floxed, shRNA-resistant MC4R-EGFP that will be produced only in cells expressing Cre recombinase (Fig. 5e). When injected into NAc of D1-Cre mice in which Cre recombinase is expressed only in D1-MSNs²⁹, robust expression of MC4R-EGFP was observed in a subpopulation of NAc cells (Fig. 5e). No expression was detected in wildtype mice injected with the same virus (Fig. 5e). The shRNA contained in this AAV was still effective in wildtype mice as evidenced by reversal of the stress-elicited weight loss (Fig. 5f) and the stress-elicited decrease in sucrose preference (Fig. 5g). In contrast, injecting this virus into NAc of stressed D1-Cre mice resulted in behavioral measurements identical to those observed in control stressed mice (Fig. 5f, g); stressed animals exhibited weight loss and decreased sucrose preference. These viral-mediated molecular manipulations had no effect on stress-elicited changes in tail suspension and forced swim tests in either wildtype or D1-Cre mice (Fig. 5h–j).

Our results thus far suggest that the synaptic modifications in the NAc that mediate chronic stress-elicited anhedonia are different than those that mediate two behaviors that are commonly used to screen compounds for antidepressant efficacy^{27, 28}. However, because only a single measure of anhedonia, the SPT, was performed it is possible that the *in vivo* molecular manipulations influenced this assay solely via effects on food intake or palatability. It was therefore important to examine whether the stress protocol and our molecular manipulations affected the “rewarding” aspect of an experience with no relationship to feeding behavior. To accomplish this goal, we determined the dose-response function for cocaine conditioned place preference (CPP), an operational measure of animals’ experience of stimuli as “rewarding”^{30, 31}. Control animals injected in NAc with AAVs

expressing GFP exhibited increases in the degree of CPP as a function of dose of cocaine received (Fig. 6a, b). In contrast, stressed animals that received NAc injections of the control AAV exhibited decreases in CPP at the lower three doses of cocaine (5, 7.5, and 10 mg/kg) but not at the highest dose (20 mg/kg) (Fig. 6a, b). These results demonstrate that stressed animals still remembered the context in which a strong “rewarding” cocaine experience occurred and therefore that the reduced CPP is due to a decreased sensitivity to cocaine reward. These stress-induced decreases in cocaine-elicited CPP were largely or entirely reversed by expression of MC4R shRNA or G2CT-Pep in the NAc (Fig. 6a, b).

Concluding remarks

Using complementary electrophysiological, molecular and behavioral approaches, we have presented evidence that during a chronic stress protocol, which elicits classic behavioral manifestations of depression in rodents, activation of MC4Rs specifically on NAc D1-MSNs leads to a depression of excitatory synaptic transmission accompanied by a change in the stoichiometry of AMPARs and that these synaptic adaptations are required for chronic stress-elicited anhedonia. Synaptic plasticity in the NAc, including modulation of LTD and LTP as well as changes in AMPAR stoichiometry, is important for several forms of psychostimulant-induced behavioral plasticity^{17, 21, 32, 33}. However, the synaptic properties being modified by the drug experience are temporally complex and depression-associated behavioral assays were not performed. Recently, evidence has accumulated that the two major subtypes of MSNs in both dorsal striatum and NAc express different synaptic properties^{12, 13} and participate in independent circuits mediating distinct behaviors. In the context of the present work, of greatest relevance are findings that independent modulation of D1-MSNs and D2-MSNs elicits different behavioral responses^{14, 15, 34}, which support the hypothesis that D1-MSN activation promotes the rewarding or incentive value of cocaine while D2-MSN activation does the opposite. Consistent with this hypothesis, inhibition of NMDAR-mediated synaptic currents in D1-MSNs attenuated cocaine reward³⁵ whereas ablation of NAc D2-MSNs enhanced amphetamine CPP³⁶. Assuming that activation of NAc D1-MSNs promotes the rewarding or incentive value of stimuli, our demonstration of a decrease in synaptic drive onto NAc D1-MSNs following chronic stress makes sense as a mechanism that importantly contributes to anhedonia. The antidepressant effect of optogenetic activation of the medial prefrontal cortex³⁷, a major input to NAc, also makes sense if this manipulation drives activity in D1-MSNs to a greater degree than D2-MSNs.

The involvement of α -MSH/MC4R signaling in NAc in triggering stress-induced synaptic adaptations provides a novel molecular mechanism by which chronic stress modulates circuitry important for reward processing and incentive salience attribution^{4–6, 38}. Perhaps of equal importance, we have provided evidence for a dissociation between the synaptic and therefore circuit modifications required for mediating stress-elicited, depression-associated anhedonia and those that mediate changes in the forced swim and tail suspension tests, behaviors that are used to predict antidepressant efficacy^{27, 28}. Synaptic adaptations in other brain areas, such as lateral habenula³⁹, may be important for these latter depression-associated behaviors. This dissociation also points out limitations of commonly used approaches to developing antidepressant medications. By delineating the molecular mechanisms underlying the circuit modifications that mediate specific behavioral

manifestations of psychiatric symptoms such as anhedonia, it should be possible to accelerate the development of efficacious therapies with novel mechanisms of action.

METHODS (for online version of paper)

Electrophysiology

Parasagittal slices (250 μm) containing the NAc core were prepared from D1-tdTomato/D2-EGFP heterozygotic BAC transgenic mice on a C57Bl6 background using standard procedures. Briefly, after mice were anesthetized with isoflurane and decapitated, brains were quickly removed and placed in ice cold low sodium, high sucrose dissecting solution. Slices were cut by adhering the two sagittal hemispheres brain containing the NAc core to the stage of a Leica vibroslicer. Slices were allowed to recover for a minimum of 60 min in a submerged holding chamber ($\sim 25^\circ\text{C}$) containing artificial cerebrospinal fluid (ACSF) consisting of 124 mM NaCl, 4.4 mM KCl, 2.5 mM CaCl_2 , 1.3 mM MgSO_4 , 1 mM NaH_2PO_4 , 11 mM glucose and 26 mM NaHCO_3 . Slices were then removed from the holding chamber and placed in the recording chamber where they were continuously perfused with oxygenated (95% O_2 , 5% CO_2) ACSF at a rate of 2 ml per min at $30 \pm 2^\circ\text{C}$. Picrotoxin (50 μM) was added to the ACSF to block GABA_A receptor-mediated inhibitory synaptic currents. Whole-cell voltage-clamp recordings from MSNs were obtained under visual control using a 63X objective. The NAc core was identified by the presence of the anterior commissure. D1- and D2 MSNs in the NAc core were identified by the presence of tdTomato and EGFP, respectively, that were excited with UV light using bandpass filters (HQ545/30x EX for tdTomato; HQ470/40x EX for EGFP). Recordings were made with electrodes (3.0–6.0 $\text{M}\Omega$) filled with 120 mM CsMeSO_4 , 15 mM CsCl, 8 mM NaCl, 10 mM HEPES, 0.2 mM EGTA, 10 mM TEACl, 4 mM MgATP , 0.3 mM NaGTP , 0.1 mM spermine and 5 mM QX-314. Excitatory afferents were stimulated with a bipolar nichrome wire electrode placed at the border between the NAc core and cortex dorsal to the anterior commissure. Recordings were performed using a Multiclamp 700B (Molecular Devices), filtered at 2 kHz and digitized at 10 kHz. EPSCs of 100–400 pA were evoked at a frequency of 0.1 Hz while MSNs were voltage-clamped at -70 mV unless otherwise stated. Data acquisition and analysis were performed on-line using custom Igor Pro software. Input resistance and access resistance were monitored continuously throughout each experiment; experiments were terminated if these changed by $>20\%$.

For monitoring α -MSH-induced synaptic changes, NAc slices were incubated in ACSF containing α -MSH (1 μM) for 2–3 h before recordings were made. Acute application of α -MSH during recordings yielded, on average, insignificant synaptic changes during 30–45 min of application. Paired-pulse ratios (PPR) were acquired by applying a second afferent stimulus of equal intensity at a specified time after the first stimulus and then calculating the ratio of EPSC2/EPSC1. For each cell for a given interstimulus interval, the PPRs of six consecutive responses were averaged. AMPAR/NMDAR ratios were calculated as the ratio of the peak amplitude of the EPSC at -70 mV (AMPA EPSCs) to the magnitude of the EPSC recorded at $+40$ mV at 50–55 ms after afferent stimulation. Miniature EPSCs were collected at a holding potential of -70 mV in the presence of TTX (0.5 μM). Thirty second blocks of events were acquired and analyzed using Mini-analysis software (Synaptosoft)

with threshold parameters set at 5 pA amplitude and <3 ms rise time. All events included in the final data analysis were verified by eye. Summary LTD graphs were generated by averaging the peak amplitudes of individual EPSCs in 1 min bins (6 consecutive sweeps) and normalizing these to the mean value of EPSCs collected during the 10 min baseline immediately before the LTD-induction protocol (3 bouts of 5 Hz stimulation for 3 min with 5 min intervals between bouts while holding cells at -50 mV)⁴⁰. Individual experiments were then averaged together. For all experiments examining LTD or the effects of α -MSH incubation, recordings from control cells were interleaved with recordings from cells undergoing the experimental manipulation with a ratio of 1 control cell for every 2–4 experimental cells. Comparisons between different experimental manipulations were made using a Mann-Whitney U-test with $P < 0.05$ considered significant. All statements in the text regarding differences between grouped data indicate that statistical significance was achieved. All values are reported as mean \pm s.e.m.

Virus and shRNA Generation

The adeno-associated viruses (AAVs) used in this study were produced by the Stanford Neuroscience Gene Vector and Virus Core. Briefly, AAV-DJ⁴¹ was produced by transfection of AAV 293 cells (Agilent, Inc) with three plasmids: an AAV vector expressing the shRNA to MC4R and EGFP or EGFP alone, AAV helper plasmid (pHELPER, Agilent, Inc), and AAV rep-cap helper plasmid (pRC-DJ, gift from Mark Kay, Stanford). At 72 h after transfection, the cells were harvested and lysed by a freeze-and-thaw procedure. Viral particles were then purified by an iodixanol step gradient ultracentrifugation method. The iodixanol was diluted and the AAV was concentrated using a 100 kDa molecular weight cutoff ultrafiltration device. The genomic titer was determined by Q-PCR. To construct short hairpin RNAs (shRNAs), oligonucleotides that contained 21 base sense and antisense sequences were connected with a hairpin loop followed by a poly(T) termination signal. The 21 base pair sequence targeting *Mc4r* (GenBank accession : NM_016977) that was used in all experiments is: GGAGAACATTCTAGTGATCGT. This shRNA was ligated into an AAV vector expressing EGFP. For initial testing of the efficacy of the shRNA, full-length mouse MC4R cDNA was fused to DsRed-monomer for fluorescent quantification of MC4R expression (MC4R-DsRed) in HEK293 cells. The plasmid expressing MC4R-DsRed was transfected and 3–4 hours later cells were infected with AAVs expressing the MC4R shRNA. Two or three days after infection, the proportion of cells expressing detectable MC4R-DsRed was determined and found to be reduced from >80% to <20% (See Supplementary Figure 4). To achieve specific MC4R expression in D1-MSNs in D1-Cre mice, we used AAV vectors with a double floxed inverted open reading frame (DIO)^{42,43}. Briefly, the EGFP tagged shRNA resistant MC4R was cloned and inserted between loxP and lox2722 sites in the reverse orientation. The resulting double floxed reverse MC4R-EGFP was cloned into AAV vectors expressing MC4R shRNA (Figure 5e).

Rabies virus (RV) was generated from a full length cDNA plasmid containing all components of RV (SAD L16; gift from Dr. Karl-Klaus Conzelmann, University of Munich, Germany)⁴⁴. We replaced the rabies virus glycoprotein with EGFP (RV-EGFP) or tdTomato (RV-tdTomato) to generate RV expressing EGFP or tdTomato. To rescue RV from this cDNA we used a modified version of a published protocol^{44,45}. Briefly, HEK293T cells

were transfected with a total of 6 plasmids; 4 plasmids expressing the RV components pTIT-N, pTIT-P, pTIT-G, and pTIT-L; one plasmid expressing T7 RNA polymerase (pCAGGS-T7), and the aforementioned glycoprotein-deleted RV cDNA plasmid expressing EGFP or tdTomato. For the amplification of RV, the media bathing these HEK293T cells was collected 3–4 days posttransfection and moved to baby hamster kidney (BHK) cells stably expressing RV glycoprotein (BHK-B19G)⁴⁶. After three days, the media from BHK-B19G cells was collected, centrifuged for 5 min at 3,000 X g to remove cell debris, and concentrated by ultracentrifugation (55,000 X g for 2 hr). Pellets were suspended in DPBS, aliquoted and stored at –80°C. The titer of concentrated RV was measured by infecting HEK293 cell and monitoring fluorescence. Plasmids expressing the RV components were gifts from Dr. Karl-Klaus Conzelmann and Dr. Ian Wickersham (Massachusetts Institute of Technology, MA). BHK cells stably expressing B19G were a gift from Dr. Edward Callaway (Salk Institute, La Jolla, CA).

Stereotaxic injections

Stereotaxic injection of viruses into NAc was performed under general ketamine-medetomidine anesthesia using a stereotaxic instrument (David Kopf). A small volume (~500 nl) of concentrated virus solution was injected unilaterally or bilaterally into NAc core (bregma 1.54 mm; lateral 1.0 mm; ventral 4.0 mm) or dorsolateral striatum (DS; bregma 0.98 mm; lateral 1.8 mm; ventral 2.2 mm) at a slow rate (100 nl/min) using a syringe pump (Harvard Apparatus, MA). The injection needle was withdrawn 5 min after the end of the infusion. Animals were used 2–3 weeks after AAV injections and 1 week after RV injections. Injection sites were confirmed in all animals by preparing coronal sections (50–100 µm) containing the dorsal striatum and NAc.

Immunohistochemistry

Immunohistochemistry and confocal microscopy were performed as described previously⁴⁷. Briefly, after intracardial perfusion with 4% paraformaldehyde in PBS (pH 7.4), the brains were fixed overnight in this same solution and coronal slices (50 µm) containing the hypothalamus were prepared. To stain for α-MSH, a rabbit anti-α-MSH (ImmunoStar, Inc.; 1:200) was applied overnight in a solution containing 1% horse serum, 0.2% BSA, and 0.5% Triton X-100 in PBS. Afterward, slices were washed four times in PBS and then incubated with the an AlexaFluor568 goat anti-rabbit secondary antibody (Molecular Probes; 1:750) for 2 h in PBS containing 0.5% Triton X-100. Subsequently, slices were washed 5 times and mounted using Vectashield mounting medium (Vector Laboratories). To identify cells expressing EGFP due to the injection of RV-EGFP into the NAc, raw EGFP fluorescence was visualized. Image acquisition was performed with a confocal microscope (Zeiss LSM510) using a 10x/0.30 Plan Neofluar and a 63x/1.40 Oil DIC Plan Apochromat objective. Confocal images were examined using the Zeiss LSM Image Browser software.

Behavioral Assays

Animals were weighed daily at the same time for three days prior to the restraint stress and throughout the restraint stress. Food intake was measured for a 24 hour period on the day before the initiation of the restraint stress and the day after the termination of the restraint stress. The Porsolt forced swim test (FST) was based on a previously described procedure⁴⁸.

At the same time each day, mice were placed individually in glass cylinders that were filled with water (25°C) to a depth that was sufficient to prevent mice from supporting themselves by placing their tails on the base of the cylinder. Each session was videotaped for offline analyses and the water was changed between each session. Immobility was defined as the lack of any swimming movements for >10 seconds. The latency to the first bout of immobility and the duration of immobility for the last 4 min of the total 6 min test period were measured.

The tail suspension test (TST) was based on a previously described procedure⁴⁸. Briefly, each mouse was individually suspended 20 cm above the floor with adhesive tape placed 1 cm from the tip of the tail. Animals were considered to be immobile when they exhibited no body movement and hung passively for >10 seconds. The time during which mice remained immobile was quantified over a period of 6 min.

For the sucrose preference tests (SPT), two water bottles were attached to cages housing individual mice. For the first 24 hours, both bottles contained water. The following day, one bottle was filled with water containing 2% sucrose and the total volume of liquid consumed from each bottle over the ensuing 24 hours was measured. The sucrose preference was calculated as the fraction of sucrose solution consumed compared to the total amount of solution consumed from both bottles. Bottles containing the sucrose solution were randomly placed on the left or right side of the compartment.

Cocaine-conditioned place preference (CPP) was conducted based on previously described procedures⁴⁹ using an open field activity chamber (ENV-510, Med Associates) equipped with infrared beams and a software interface (Activity Monitor, Med Associates) that monitors the position of the mouse⁵⁰. The apparatus was divided into two equally sized zones using plastic floor tiles with distinct visual and tactile cues (grey & smooth or white & rough). The amount of time spent freely exploring each zone was recorded during 20 minute test sessions. After an initial test to establish baseline preference for the two sets of cues, each mouse was randomly assigned in a counterbalanced fashion to receive cocaine in the presence of one set of cues (i.e., an unbiased design). Four conditioning cycles were conducted with ascending doses of cocaine (5, 7.5, 10, and 20 mg/kg). Each cycle began with an i.p. injection of saline and exposure to the appropriate set of cues for 20 minutes. A second conditioning session with cocaine was conducted 2–4 hours later in the presence of the other set of cues. A test session was conducted the day after conditioning to determine time spent in the presence of the cocaine-associated cues (i.e., CPP), while the next cycle of conditioning commenced the following day. This protocol allowed us to determine a dose-response function for cocaine CPP in each individual subject, providing enhanced resolution for detecting shifts in cocaine sensitivity caused by stressful experience and viral-mediated molecular manipulations.

Measurement of MC4R expression in NAc

NAc tissue surrounding the anterior commissure was dissected from freshly isolated brain slices and rapidly frozen in liquid nitrogen. This tissue was then lysed in ice-cold homogenate buffer (50 mM Tris-HCl, 150 mM NaCl, Nonidet P40, 0.5% sodium deoxycholate, pH7.5) containing a protease inhibitor cocktail (Roche Applied Science) and

homogenized. The protein concentration of the lysates was measured using the Bradford method (Bio-rad) and 50 µg of lysates was used for analysis. Samples were separated on 4–12% gradient Bis-Tris gels (Invitrogen) and transferred onto nitrocellulose membranes. After transfer, the membranes were blocked with 5% milk in 0.1M PBS and incubated overnight at 4°C with rabbit polyclonal MC4R antibody (Abcam) or mouse monoclonal β -tubulin antibody (Abcam). After washing five times with PBS containing 0.5% Tween-20, the membrane was incubated with horseradish peroxidase-conjugated anti-rabbit or anti-mouse secondary antibody (1:5000, Sigma) for 1 h. The immunoreactive bands were visualized using an ECL chemiluminescence reagent (GE Healthcare) according to the manufacturer's instructions. The scanned digital images were used for quantification. For comparing the levels of MC4Rs, the intensity of MC4R signals was normalized to the intensity of the β -tubulin signal.

Supplementary Material

Refer to Web version on PubMed Central for supplementary material.

Acknowledgements

We thank J. Kauer, D. Lyons and members of the Malenka laboratory for helpful comments. The rabies virus cDNA plasmid and viral component-expressing plasmids were gifts from K. Conzelmann (University of Munich, Germany) and I. Wickersham (MIT, MA). BAC-transgenic mice were generously provided by N. Calakos (Duke University, NC). BHK-B19G cells were a gift from E. Callaway (Salk Institute, CA). The AAVs used in this study were produced by the Stanford Neuroscience Gene Vector and Virus Core. The AAV-DJ helper plasmid was a gift from Mark Kay (Stanford, CA). B. K. L is supported by a Davis Foundation Postdoctoral Fellowship in Eating Disorders Research. We acknowledge funding from the N.I.H. (R.C.M.).

References

1. Cone RD. Anatomy and regulation of the central melanocortin system. *Nat. Neurosci.* 2005; 8:571–578. [PubMed: 15856065]
2. Gao Q, Horvath TL. Neurobiology of feeding and energy expenditure. *Annu. Rev. Neurosci.* 2007; 30:367–398. [PubMed: 17506645]
3. Morton GJ, Cummings DE, Baskin DG, Barsh GS, Schwartz MW. Central nervous system control of food intake and body weight. *Nature.* 2006; 443:289–295. [PubMed: 16988703]
4. Kelley AE, Berridge KC. The neuroscience of natural rewards: relevance to addictive drugs. *J. Neurosci.* 2002; 22:3306–3311. [PubMed: 11978804]
5. Volkow ND, Wang GJ, Baler RD. Reward, dopamine and the control of food intake: implications for obesity. *Tr. Cogn. Sci.* 2011; 15:37–46.
6. Nestler EJ, Carlezon WA Jr. The mesolimbic dopamine reward circuit in depression. *Biol. Psychiatry.* 2006; 59:1151–1159. [PubMed: 16566899]
7. Liu J, et al. The melanocortinergic pathway is rapidly recruited by emotional stress and contributes to stress-induced anorexia and anxiety-like behavior. *Endocrinology.* 2007; 148:5531–5540. [PubMed: 17673512]
8. Hsu R, et al. Blockade of melanocortin transmission inhibits cocaine reward. *Eur. J. Neurosci.* 2005; 21:2233–2242. [PubMed: 15869520]
9. Chaki S, Ogawa S, Toda Y, Funakoshi T, Okuyama S. Involvement of the melanocortin MC4 receptor in stress-related behavior in rodents. *Eur. J. Pharmacol.* 2003; 474:95–101. [PubMed: 12909200]
10. Chaki S, Okuyama S. Involvement of melanocortin-4 receptor in anxiety and depression. *Peptides.* 2005; 26:1952–1964. [PubMed: 15979204]

11. Shuen JA, Chen M, Gloss B, Calakos N. *Drd1a-tdTomato* BAC transgenic mice for simultaneous visualization of medium spiny neurons in the direct and indirect pathways of the basal ganglia. *J. Neurosci.* 2008; 28:2681–2685. [PubMed: 18337395]
12. Kreitzer AC, Malenka RC. Striatal plasticity and basal ganglia circuit function. *Neuron.* 2008; 60:543–554. [PubMed: 19038213]
13. Grueter BA, Brasnjo G, Malenka RC. Postsynaptic TRPV1 triggers cell type-specific long-term depression in the nucleus accumbens. *Nat. Neurosci.* 2010; 13:1519–1525. [PubMed: 21076424]
14. Lobo MK, et al. Cell type-specific loss of BDNF signaling mimics optogenetic control of cocaine reward. *Science.* 2010; 330:385–390. [PubMed: 20947769]
15. Hikida T, Kimura K, Wada N, Funabiki K, Nakanishi S. Distinct roles of synaptic transmission in direct and indirect striatal pathways to reward and aversive behavior. *Neuron.* 2010; 66:896–907. [PubMed: 20620875]
16. Kauer JA, Malenka RC. Synaptic plasticity and addiction. *Nat. Rev. Neurosci.* 2007; 8:844–858. [PubMed: 17948030]
17. Conrad KL, et al. Formation of accumbens GluR2-lacking AMPA receptors mediates incubation of cocaine craving. *Nature.* 2008; 454:118–121. [PubMed: 18500330]
18. Isaac JT, Ashby MC, McBain CJ. The role of the GluR2 subunit in AMPA receptor function and synaptic plasticity. *Neuron.* 2007; 54:859–871. [PubMed: 17582328]
19. Brog JS, Salyapongse A, Deutch AY, Zahm DS. The patterns of afferent innervation of the core and shell in the "accumbens" part of the rat ventral striatum: immunohistochemical detection of retrogradely transported fluoro-gold. *J. Comp. Neurol.* 1993; 338:255–278. [PubMed: 8308171]
20. Wickersham IR, Finke S, Conzelmann KK, Callaway EM. Retrograde neuronal tracing with a deletion-mutant rabies virus. *Nat. Methods.* 2007; 4:47–49. [PubMed: 17179932]
21. Brebner K, et al. Nucleus accumbens long-term depression and the expression of behavioral sensitization. *Science.* 2005; 310:1340–1343. [PubMed: 16311338]
22. Shepherd JD, Huganir RL. The cell biology of synaptic plasticity: AMPA receptor trafficking. *Annu.Rev. Cell Devel. Biol.* 2007; 23:613–643. [PubMed: 17506699]
23. Lee SH, Liu L, Wang YT, Sheng M. Clathrin adaptor AP2 and NSF interact with overlapping sites of GluR2 and play distinct roles in AMPA receptor trafficking and hippocampal LTD. *Neuron.* 2002; 36:661–674. [PubMed: 12441055]
24. Yang Y. Structure, function and regulation of the melanocortin receptors. *Eur. J. Pharmacol.* 2011; 660:125–130. [PubMed: 21208602]
25. Woolfrey KM, et al. Epac2 induces synapse remodeling and depression and its disease-associated forms alter spines. *Nat. Neurosci.* 2009; 12:1275–1284. [PubMed: 19734897]
26. Bos JL. Epac proteins: multi-purpose cAMP targets. *Tr. Biochem. Sci.* 2006; 31:680–686.
27. Nestler EJ, Hyman SE. Animal models of neuropsychiatric disorders. *Nat. Neurosci.* 2010; 13:1161–1169. [PubMed: 20877280]
28. Porsolt RD, Brossard G, Hautbois C, Roux S. Rodent models of depression: forced swimming and tail suspension behavioral despair tests in rats and mice. *Curr. Protoc. Neurosci.* 2001; Chapter 8(Unit 8):10A.
29. Gong S, et al. Targeting Cre recombinase to specific neuron populations with bacterial artificial chromosome constructs. *J. Neurosci.* 2007; 27:9817–9823. [PubMed: 17855595]
30. Bardo MT, Bevins RA. Conditioned place preference: what does it add to our preclinical understanding of drug reward? *Psychopharmacology (Berl).* 2000; 153:31–43. [PubMed: 11255927]
31. Cunningham CL, Gremel CM, Groblewski PA. Drug-induced conditioned place preference and aversion in mice. *Nat. Protoc.* 2006; 1:1662–1670. [PubMed: 17487149]
32. Kasanetz F, et al. Transition to addiction is associated with a persistent impairment in synaptic plasticity. *Science.* 2010; 328:1709–1712. [PubMed: 20576893]
33. Pascoli V, Turiault M, Luscher C. Reversal of cocaine-evoked synaptic potentiation resets drug-induced adaptive behaviour. *Nature.* 2011; 481:71–75. [PubMed: 22158102]
34. Ferguson SM, et al. Transient neuronal inhibition reveals opposing roles of indirect and direct pathways in sensitization. *Nat Neurosci.* 2011; 14:22–24. [PubMed: 21131952]

35. Heusner CL, Palmiter RD. Expression of mutant NMDA receptors in dopamine D1 receptor-containing cells prevents cocaine sensitization and decreases cocaine preference. *J. Neurosci.* 2005; 25:6651–6657. [PubMed: 16014726]
36. Durieux PF, et al. D2R striatopallidal neurons inhibit both locomotor and drug reward processes. *Nat Neurosci.* 2009; 12:393–395. [PubMed: 19270687]
37. Covington HE 3rd, et al. Antidepressant effect of optogenetic stimulation of the medial prefrontal cortex. *J. Neurosci.* 2010; 30:16082–16090. [PubMed: 21123555]
38. Berridge KC, Robinson TE, Aldridge JW. Dissecting components of reward: 'liking', 'wanting', and learning. *Curr. Opin. Pharmacol.* 2009; 9:65–73. [PubMed: 19162544]
39. Li B, et al. Synaptic potentiation onto habenula neurons in the learned helplessness model of depression. *Nature.* 2011; 470:535–539. [PubMed: 21350486]

References

40. Thomas MJ, Beurrier C, Bonci A, Malenka RC. Long-term depression in the nucleus accumbens: a neural correlate of behavioral sensitization to cocaine. *Nat. Neurosci.* 2001; 4:1217–1223. [PubMed: 11694884]
41. Grimm D, et al. In vitro and in vivo gene therapy vector evolution via multispecies interbreeding and retargeting of adeno-associated viruses. *J. Virol.* 2008; 82:5887–5911. [PubMed: 18400866]
42. Atasoy D, Aponte Y, Su HH, Sternson SM. A FLEX switch targets Channelrhodopsin-2 to multiple cell types for imaging and long-range circuit mapping. *J. Neurosci.* 2008; 28:7025–7030. [PubMed: 18614669]
43. Tsai HC, Zhang F, Adamantidis A, Stuber GD, Bonci A, de Lecea L, Deisseroth K. Phasic firing in dopaminergic neurons is sufficient for behavioral conditioning. *Science.* 2009; 324:1080–1084. [PubMed: 19389999]
44. Mebatsion T, König M, Conzelmann KK. Budding of rabies virus particles in the absence of the spike glycoprotein. *Cell.* 1996; 84:941–951. [PubMed: 8601317]
45. Wickersham IR, Sullivan HA, Seung HS. Production of glycoprotein-deleted rabies viruses for monosynaptic tracing and high-level gene expression in neurons. *Nat. Protoc.* 2010; 5:595–606. [PubMed: 20203674]
46. Wickersham IR, Finke S, Conzelmann KK, Callaway EM. Retrograde neuronal tracing with a deletion-mutant rabies virus. *Nat. Methods.* 2007; 4:47–49. [PubMed: 17179932]
47. Wolfart J, Neuhoff H, Franz O, Roeper J. Differential expression of the small-conductance, calcium-activated potassium channel SK3 is critical for pacemaker control in dopaminergic midbrain neurons. *J. Neurosci.* 2001; 21:3443–3456. [PubMed: 11331374]
48. Porsolt RD, Brossard G, Hautbois C, Roux S. Rodent models of depression: forced swimming and tail suspension behavioral despair tests in rats and mice. *Curr. Protoc. Neurosci.* 2001; Chapter 8(Unit 8)
49. Cunningham CL, Gremel CM, Groblewski PA. Drug-induced conditioned place preference and aversion in mice. *Nat. Protoc.* 2006; 1:1662–1670. [PubMed: 17487149]
50. Grueter BA, Brasnjo G, Malenka RC. Postsynaptic TRPV1 triggers cell type-specific long-term depression in the nucleus accumbens. *Nat. Neurosci.* 2010; 13:1519–1525. [PubMed: 21076424]

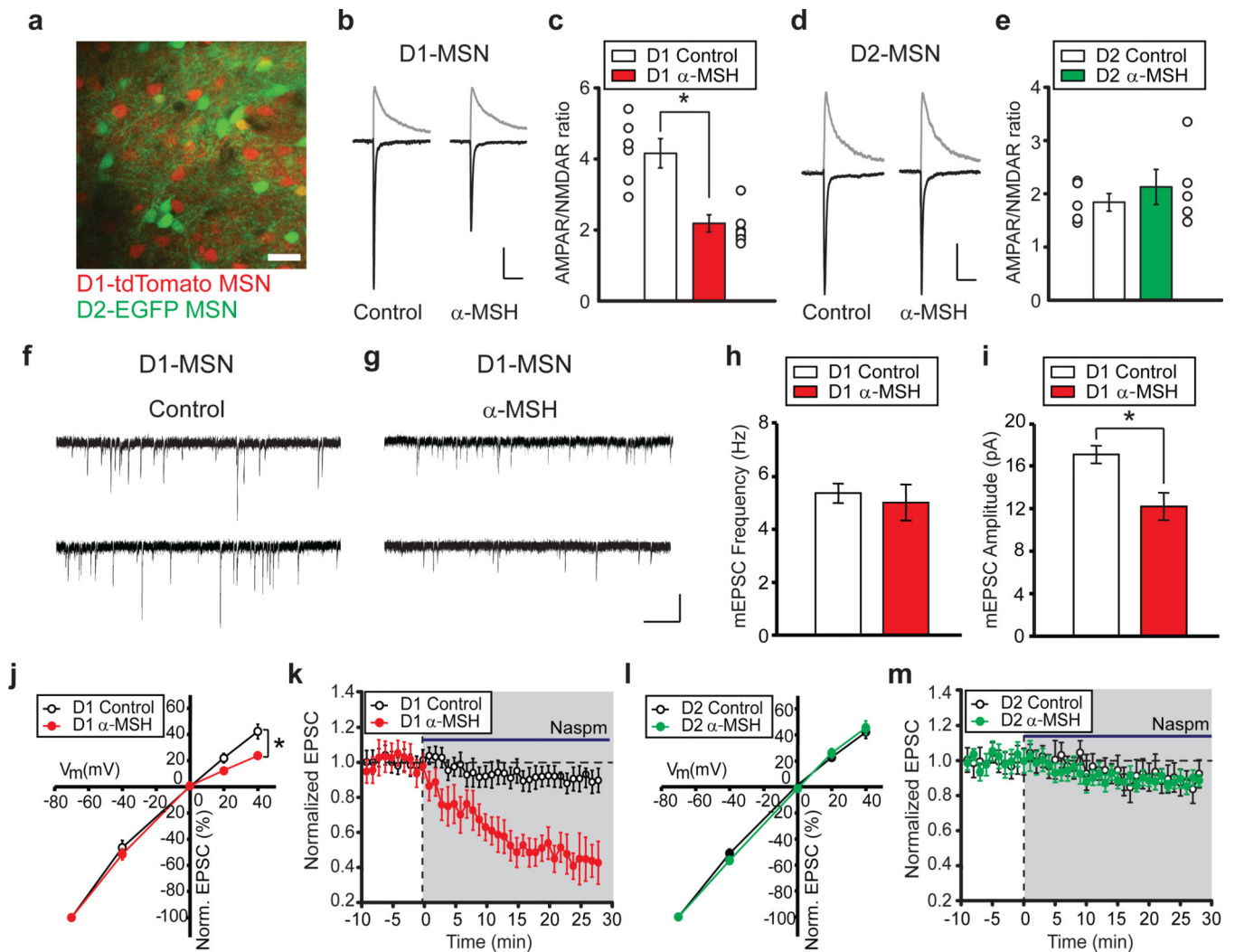


Figure 1. α -MSH modifies excitatory synapses on NAc D1-MSNs

a, Image of NAc slice from *Drd1a-tdTomato/Drd2-EGFP* BAC transgenic mouse (scale bar, 50 μ m). **b, c**, D1-MSN EPSCs at -70 mV and $+40$ mV (**b**) and summary (**c**) of α -MSH effects on AMPAR/NMDAR ratios (Control, 4.16 ± 0.35 , $n = 7$; α -MSH, 2.18 ± 0.29 , $n = 8$; $*P < 0.05$ Mann-Whitney U-test; error bars are s.e.m. in all figures). Scale bars: 60, 70 pA/100 ms. **d, e**, EPSCs from D2-MSNs (**d**) and summary (**e**) showing no effect of α -MSH (Control, 1.86 ± 0.25 , $n = 6$; α -MSH, 2.12 ± 0.34 , $n = 5$). Scale bars: 90, 100 pA/100 ms. **f, g**, mEPSCs from control D1-MSN (**f**) or D1-MSN exposed to α -MSH (**g**) Scale bars: 20 pA/0.5 s. **h, i**, Summary of α -MSH effects on mEPSC frequency (**h**; Control, 5.3 ± 0.4 Hz, $n = 9$; α -MSH, 5.0 ± 0.7 Hz, $n = 11$) and amplitude (**i**; Control, 17.1 ± 0.8 pA; α -MSH, 12.2 ± 1.2 pA; $*P < 0.05$ Mann-Whitney U-test). **j–m**, Effects of α -MSH on AMPAR stoichiometry. AMPAR EPSC amplitudes at different membrane potentials (**j**) (normalized to -70 mV) show α -MSH increases AMPAR EPSC rectification in D1-MSNs (Control, $n = 9$; α -MSH, $n = 12$, $*P < 0.05$ Mann-Whitney U-Test) and enhances effects of Naspm (200 μ M) (**k**, Control: $89 \pm 4\%$, $n = 6$; α -MSH: $47 \pm 9\%$ of baseline 20–25 min after Naspm application, $n = 8$; $*P < 0.05$ Mann-Whitney U-Test). In D2-MSNs α -MSH does not affect

AMPA EPSC rectification (**l**, Control, $n = 8$; α -MSH, $n = 8$) nor the Nasp^m-induced depression (**m**, Control: $91 \pm 5\%$, $n = 6$; α -MSH: $90 \pm 4\%$, $n = 7$).

Author Manuscript

Author Manuscript

Author Manuscript

Author Manuscript

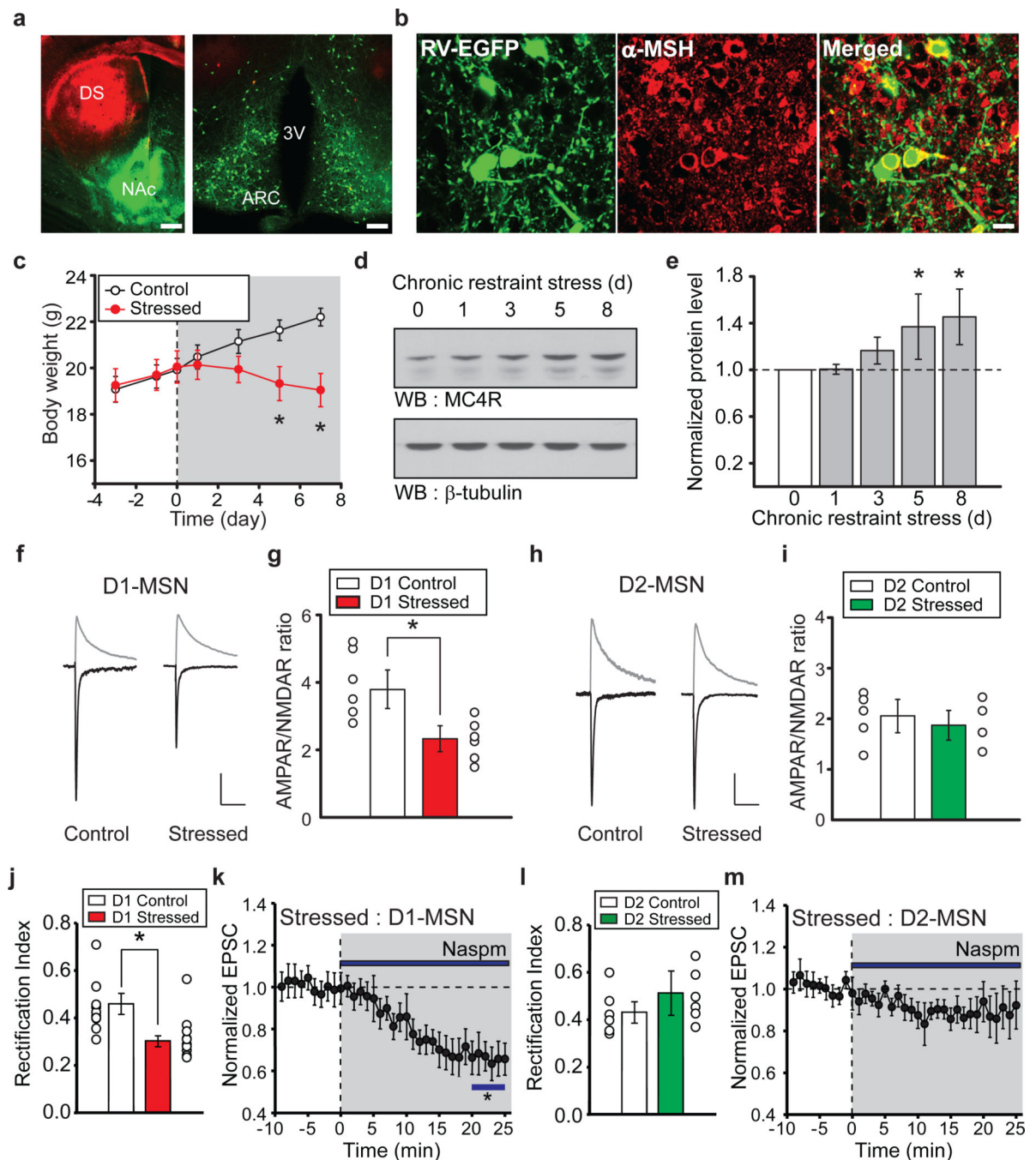


Figure 2. Chronic restraint stress modifies excitatory synapses on NAc D1-MSNs

a, Coronal sections of dorsal striatum (DS) and NAc (left panel: scale bar, 500 μ m) and retrogradely labeled cells in hypothalamus (right panel: ARC, arcuate nucleus; 3V, third ventricle; scale bar, 200 μ m) 1 week following injections of RV-EGFP into NAc and RV-tdTomato into DS. **b**, ARC neurons retrogradely labeled by RV-EGFP injected into the NAc and immunostained for α -MSH (scale bar, 20 μ m). **c**, Body weight of control mice ($n=12$) and mice subjected to restraint stress ($n=15$; $*P < 0.05$ Mann-Whitney U-Test). **d**, **e**, Western blots (**d**) and quantification (**e**) showing changes in MC4R levels in NAc during

restraint stress (8th day of restraint stress, NAc MC4R levels are $143 \pm 14\%$ of control NAc MC4R levels, $n = 3$, $*P < 0.05$ Mann-Whitney U-Test). **f-i**, Effects of restraint stress on AMPAR/NMDAR ratios in D1-MSNs and D2-MSNs. EPSCs at -70 mV and $+40$ mV from D1-MSNs (**f**) and summary (**g**) showing stress-induced decrease in AMPAR/NMDAR ratios (Control, 3.77 ± 0.59 , $n = 6$; Stressed, 2.34 ± 0.36 , $n = 6$; $*P < 0.05$ Mann-Whitney U-Test). EPSCs (**h**) and summary (**i**) of AMPAR/NMDAR ratios from D2-MSNs (Control, 2.03 ± 0.32 , $n = 5$; Stressed, 1.88 ± 0.29 , $n = 4$). Scale bars in f: 80, 100 pA/100 ms. Scale bars in h: 90, 110 pA/100 ms. **j-m**, Restraint stress changes AMPAR stoichiometry in D1-MSNs but not D2-MSNs. Rectification index of AMPAR EPSCs in D1-MSNs (**j**) (Control, 0.46 ± 0.04 , $n = 8$; Stressed: 0.29 ± 0.02 , $n = 10$; $*P < 0.05$ Mann-Whitney U-test). Effect of Nasp^m (**k**) on D1-MSN AMPAR EPSCs from stressed animals ($65 \pm 8\%$, $n = 7$; $*P < 0.05$ Mann-Whitney U-Test). Restraint stress has no effect on D2-MSN AMPAR EPSC rectification (**l, m**) (Control rectification index, 0.43 ± 0.04 , $n = 6$; Stressed: 0.51 ± 0.09 , $n = 6$; Nasp^m, sensitivity, $88 \pm 11\%$, $n = 6$).

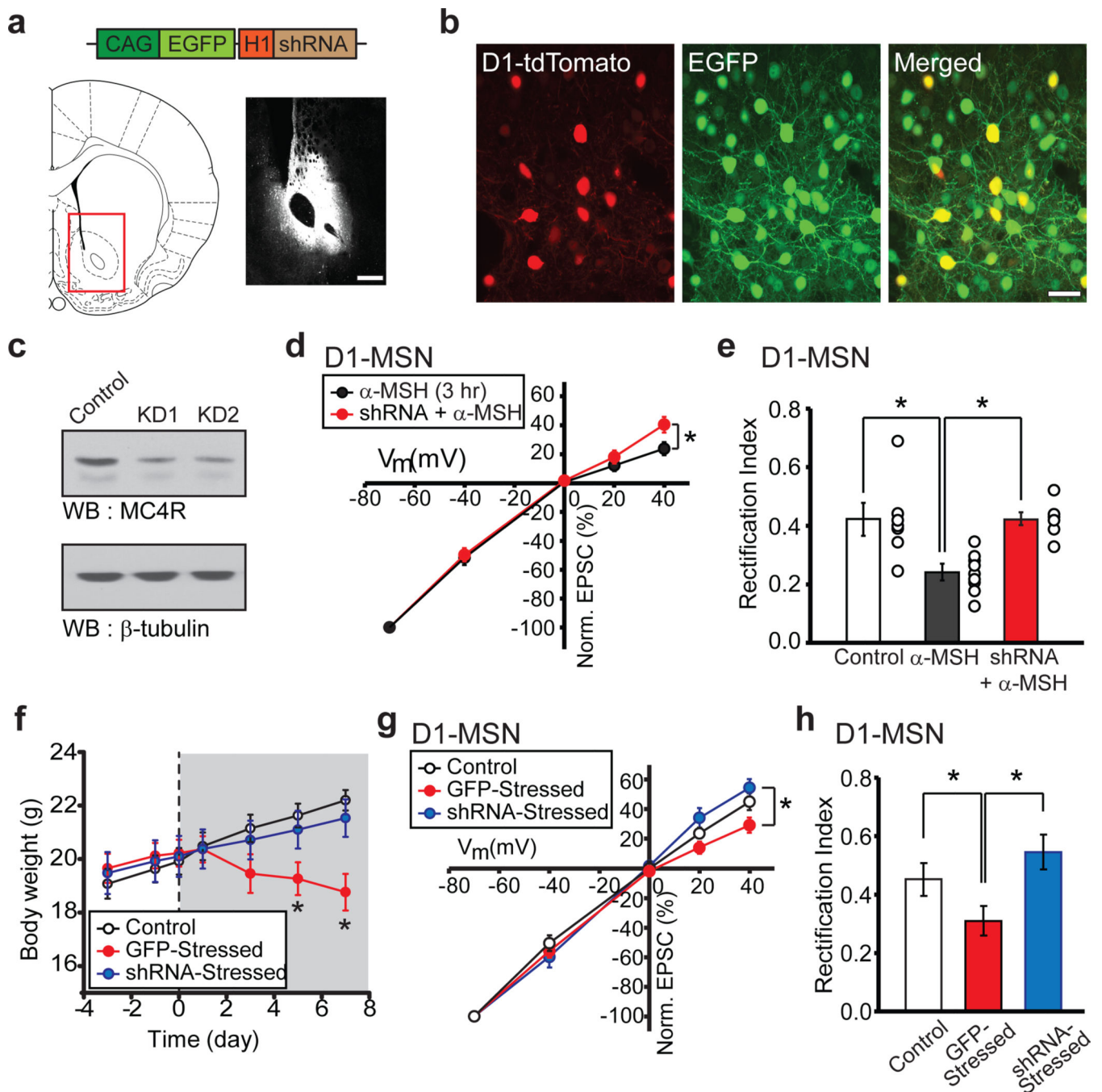


Figure 3. Knockdown of NAc MC4Rs prevents stress-induced weight loss and synaptic changes
a, Schematics of AAV vector expressing MC4R shRNA (top) and injection site into NAc core (red box, lower left) with image of EGFP expression in NAc core 2 weeks following injection (lower right; scale bar, 500 μ m). **b**, Magnified images showing EGFP expression in NAc D1-tdTomato MSNs 2 weeks after injection of AAV-MC4R shRNA (scale bar, 20 μ m). **c**, MC4R Western blots from NAc of two animals injected with AAV-MC4R shRNA. **d,e**, D1-MSN AMPAR EPSC amplitudes at different membrane potentials (**d**) and rectification index (**e**, Control: 0.42 ± 0.06 , $n = 7$; α -MSH: 0.24 ± 0.02 , $n = 9$; shRNA + α -

MSH: 0.43 ± 0.02 , $n = 6$; $*P < 0.05$ Mann-Whitney U-Test) demonstrating that *in vivo* MC4R shRNA prevents the α -MSH-induced change in D1-MSN AMPAR EPSC rectification. **f**, Stress-induced decrease in body weight is prevented by knockdown of NAc MC4Rs but not by injection of control AAV expressing GFP (Control, $n = 12$; GFP-Stressed, $n = 9$; shRNA-Stressed, $n = 12$; $*P < 0.05$ Mann-Whitney U-Test). **g, h**, D1-MSN AMPAR EPSC amplitudes at different membrane potentials (**g**) and rectification index (**h**, Control, 0.42 ± 0.06 , $n = 7$ [same as in **e**]; GFP-Stressed, 0.31 ± 0.05 , $n = 6$; shRNA - Stressed, 0.54 ± 0.08 , $n = 7$; $*P < 0.05$ Mann-Whitney U-Test) showing that *in vivo* knockdown of NAc MC4Rs prevents the stress-induced increase in D1-MSN AMPAR EPSC rectification.

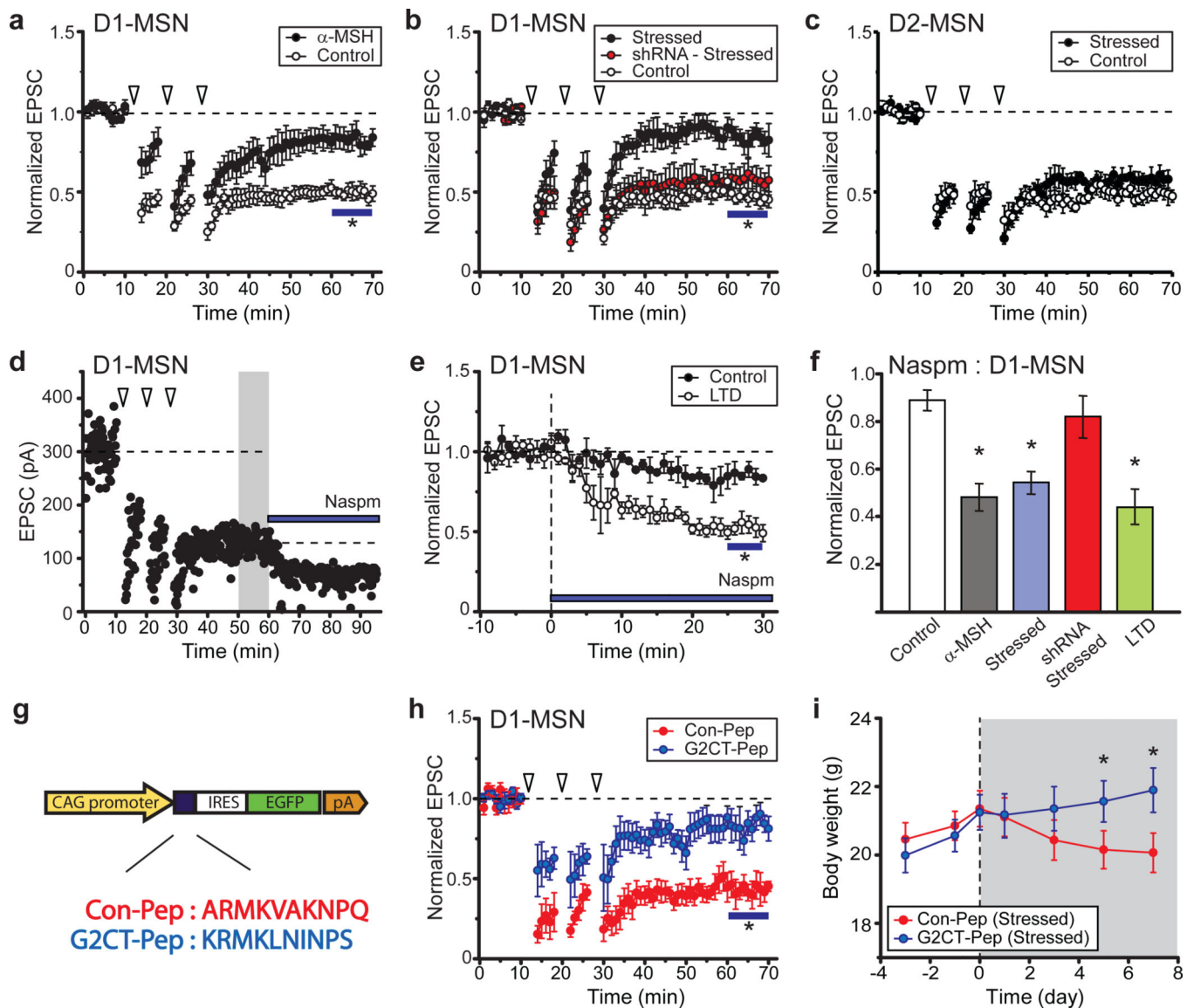


Figure 4. Chronic restraint stress induces “LTD” in D1-MSNs

a, Prior exposure to α -MSH reduces NMDAR-dependent LTD in NAc D1-MSNs (Control, $47 \pm 4\%$ of baseline 50–60 min after start of induction protocol, $n = 7$; α -MSH, $82 \pm 6\%$, $n = 5$; * $P < 0.05$ Mann-Whitney U-Test) **b**, LTD in D1-MSNs is reduced by restraint stress (Control, $46 \pm 5\%$, $n = 8$; Stressed, $84 \pm 7\%$, $n = 11$; * $P < 0.05$ Mann-Whitney U-Test) and this decrease is prevented by *in vivo* knockdown of NAc MC4Rs (shRNA-Stressed, $0.58 \pm 9\%$, $n = 7$). **c**, LTD in D2-MSNs is not affected by restraint stress (Control, $49 \pm 3\%$, $n = 7$; Stressed, $54 \pm 5\%$, $n = 6$). **d**, **e**, Sample experiment (**d**) and summary (**e**) showing that following LTD induction, effects of Naspms are increased (Control, $85 \pm 5\%$ of baseline, $n = 6$; $51 \pm 4\%$, $n = 4$). **f**, Effects of Naspms on D1-MSN AMPAR EPSCs following various experimental manipulation (* $P < 0.05$ compared to control, Mann-Whitney U-test) **g**, Schematic of AAV-vector expressing control peptide (Con-Pep) or peptide blocking GluA2 binding to AP2 (G2CT-Pep). **h**, LTD in D1-MSNs is reduced by *in vivo* expression of

G2CT-Pep ($81 \pm 7\%$ of baseline, $n = 6$) but not Con-pep ($47 \pm 5\%$, $n = 5$; $*P < 0.05$ Mann-Whitney U-Test). **i**, Stress-induced decrease in body weight is prevented by expression of G2CT-Pep in NAc ($n = 10$) but not by Con-Pep expression ($n = 9$; $*P < 0.05$ Mann-Whitney U-Test).

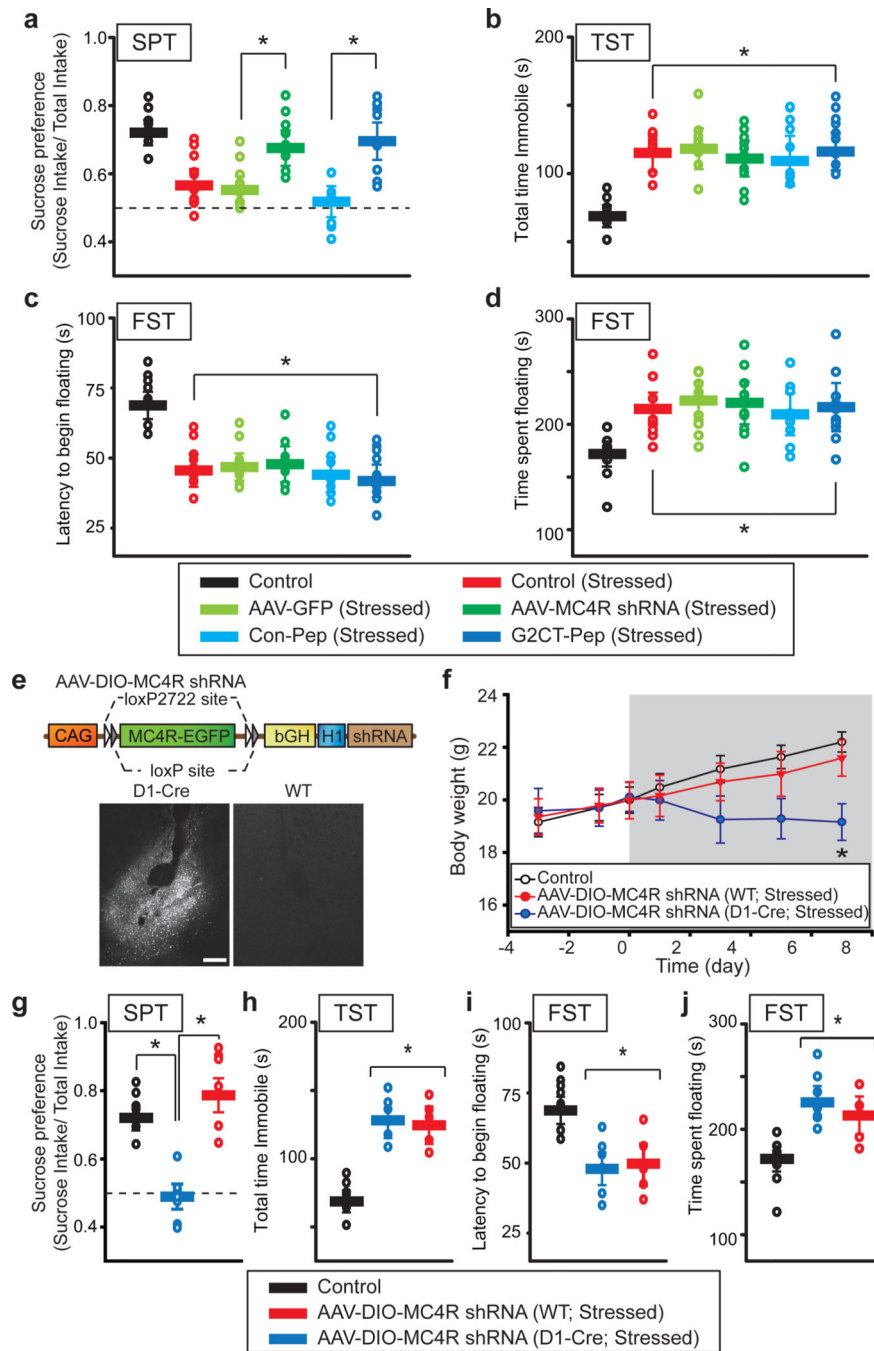


Figure 5. MC4R activation and LTD in the NAc are required for stress-induced anhedonia
a, Summary of the sucrose preference test in control mice ($n = 9$), mice subjected to restraint stress ($n = 9$) and stressed mice who received NAc injections of AAVs expressing GFP alone ($n = 9$), MC4R shRNA ($n = 10$), Con-Pep ($n = 8$) or G2CT-Pep ($n = 10$). Expression of either MC4R shRNA or G2CT-Pep in NAc prevented the stress-induced change in this test (* $P < 0.05$ Mann-Whitney U-Test). **b**, In the tail suspension tests, these same animals showed a stress-induced increase in time spent immobile (* $P < 0.05$ Mann-Whitney U-Test compared to Control). **c**, **d**, Animals also showed stress-induced changes in the forced swim

test measured by latency to the first bout of immobile floating (**c**) or total duration of immobility/floating (**d**) (* $P < 0.05$ Mann-Whitney U-Test compared to Control). **e**. Diagram of AAV vector used to rescue MC4R in D1-MSNs only. Images of MC4R-EGFP expression following injection of virus into NAc core of D1-Cre mice and wildtype (WT) mice. Scale bar: 250 μm . **f**. Reversal of stress-induced decrease in body weight by knockdown of NAc MC4Rs was prevented by D1-MSN specific expression of shRNA resistant MC4R (Control, $n = 12$; AAV-DIO-MC4R shRNA (WT), $n = 8$; AAV-DIO-MC4R shRNA (D1-Cre), $n = 7$; * $P < 0.05$ Mann-Whitney U-Test). **g–j**. Summary of the sucrose preference test (**g**), tail suspension test (**h**) and forced swim test (**i–j**) in control mice, stressed wild-type and stressed D1-Cre mice. Both groups of stressed mice received NAc injections of AAV-DIO-MC4R shRNAs. D1-MSN specific rescue of MC4Rs reversed the effects of the MC4R shRNA in the sucrose preference test but had no effect on the tail suspension and forced swim tests (* $P < 0.05$ Mann-Whitney U-Test).

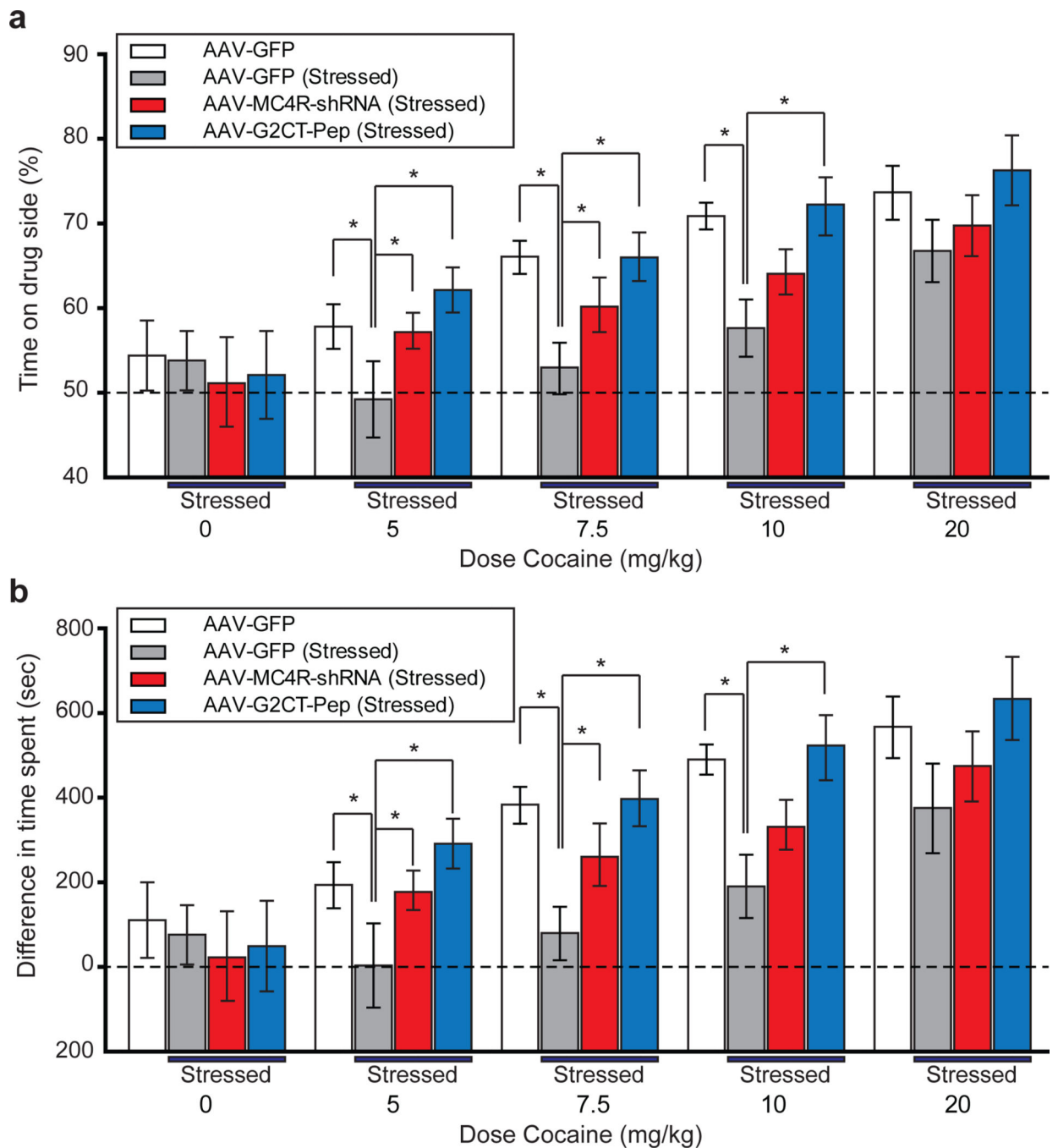


Figure 6. MC4R activation and LTD in the NAc are required for stress-induced decreases in cocaine conditioned place preference (CPP)

a,b. CPP induced by different doses of cocaine in mice that received NAc injection of AAV expressing GFP alone ($n = 6$), and stressed mice who received NAc injections of AAVs expressing GFP alone ($n = 6$), MC4R shRNA ($n = 7$), or G2CT-Pep ($n = 6$). CPP was measured as percentage of time spent on the cocaine-paired side (**a**), and the differences between time spent on cocaine-conditioned and saline-conditioned sides (**b**). Stress reduced CPP at the three lower doses but not the highest dose (20 mg/kg) and this decrease was

prevented by expression of MC4R shRNA and G2CT-Pep (* $P < 0.05$ Mann-Whitney U-Test).

Author Manuscript

Author Manuscript

Author Manuscript

Author Manuscript